

Hendrik D. Visse

Catalysis of CO oxidation using the kinetic Monte Carlo method

Bachelor thesis
June 21th, 2012

Supervisors:
prof. dr. J.W.M. Frenken
prof. dr. E.A. Verbitskiy



LION / Mathematisch Instituut
Universiteit Leiden

*Non è il mondan romore altro ch'un fiato
di vento, ch'or vien quinci e or vien quindi,
e muta nome perché muta lato.*

— Dante Alighieri, *Purgatorio*,
Canto XI, lines 100-102

Abstract

The oxidation of CO on the Pd(100)($\sqrt{5} \times \sqrt{5}$) $R27^\circ$ surface is studied using the kinetic Monte Carlo simulation method. The occupation by oxygen of a specific type of site – the hollow sites – is monitored in order to gain insight into experiments on the restructuring of the surface which itself might be a explanation of oscillations measured in the reactivity in the oxidation reaction. Two indications have been found that oxygen atoms will only vacate the hollow sites that are they normally occupy in a clean oxidized surface if their place is taken by CO molecules.

Contents

| | | |
|-----------|---|-----------|
| 1 | Introduction | 4 |
| 1.1 | Oscillations in catalysis | 4 |
| 1.2 | Reaction mechanisms | 4 |
| 2 | CO oxidation on Pd(100) | 6 |
| 2.1 | Lattice structure | 6 |
| 2.2 | Role of oxide | 6 |
| 3 | Kinetic Monte Carlo | 7 |
| 3.1 | Choosing a process | 7 |
| 3.2 | Handling the time parameter | 8 |
| 3.3 | The rates | 8 |
| 3.3.1 | Formulas | 8 |
| 3.3.2 | Values | 9 |
| 4 | Results of Rogal, Reuter and Scheffler | 12 |
| 5 | Simulations | 15 |
| 5.1 | Full model | 15 |
| 5.2 | To study the rarer processes | 17 |
| 5.2.1 | Handling CO and problems | 18 |
| 6 | Intermezzo: The entropy effect | 21 |
| 7 | Reducing the model | 22 |
| 7.1 | Further simplification | 22 |
| 7.2 | Differential equations | 23 |
| 8 | Discussion and outlook | 25 |
| 9 | Conclusion | 25 |
| 10 | Acknowledgements | 25 |
| | References | 26 |

1 Introduction

1.1 Oscillations in catalysis

Catalysts have been under study for quite some time now. An obvious reason for this is the technological applications that catalysis can yield. Besides these applications there is a more fundamental reason for studying catalysis which is that even catalysts that have been in practical use for some time are still poorly understood. Research on catalysis is typically performed at low pressures. Only recently have scientist been able to study catalysts under conditions similar to those in technological applications, in real life [4].

A major open problem in the field of catalysis is that of oscillations in the reaction rate. Oscillatory behaviour in the reaction rate of CO oxidation on platinum, palladium and iridium has been observed as early as 1970s and 1980s. An excellent report on this is [12] whose authors Sales, Turner and Maple [10] have proposed in 1982 that oxide forming on metal surfaces kills the catalytic reaction and that this was the cause for oscillations. However, this claim has not been free from critics. For several years now research has shown that oxides can in fact be extremely good catalysts. [3] Recent studies have shown that the transition from an oxidized surface to a clean surface and the transition back may cause the oscillatory behaviour [13]. However, it is quite possible that there is still more to find out about these oscillations as the topic is highly debated by several research teams and consensus has not yet been reached [2].

In this thesis by catalysis, we will always refer to heterogeneous catalysis, in which a solid acts as a catalyst for reactants in a surrounding gaseous mixture.

1.2 Reaction mechanisms

There are three main mechanisms for particles to interact with a catalytic surface: the Langmuir-Hinshelwood mechanism, the Eley-Rideal mechanism and the Mars-Van Krevelen mechanism. We will discuss each of them shortly.

- In the Langmuir-Hinshelwood mechanism [1] both reactants adsorb to the catalytic surface on which they stay for a short while. When two different reactant particles meet as neighbours, for example, by adsorbing on the correct sites, or by diffusing to them, they have a non-zero probability to react and form a product, which then can either stay on the surface or leave it as part of the modeled process.
- In the Eley-Rideal mechanism [1] only one of the reactant particles has to adsorb to the surface where it patiently awaits the arrival of a particle of the second reactant in the surrounding gas or liquid. These can then react and the product is removed from the surface immediately.
- The Mars-Van Krevelen mechanism [5] is somewhat a mixture of the two above. One of the reactants is considered to be part of the surface while the second reactant reacts with the first directly from the mixture. The particle from the surface is then replaced by a new particle from either the bulk of the catalyst or the gas phase [4].

In our model we assume the Langmuir-Hinshelwood mechanism in the sense that each of the particles involved in the reaction occupies an adsorption site (of which we have two types, see section 2.1). In order for a CO molecule and an O atom to react and form a CO₂ molecule, both must be adsorbed to the surface. Carbonmonoxide adsorbs in a single piece. An oxygen O₂ molecule adsorbes dissociatively, that is, it breaks apart into two separate oxygen atoms, both of which must adsorb on available surface sites. For each of these adsorption processes, we also consider the accompanying desorption processes. Furthermore we consider diffusion

processes of both O and CO from one site to a neighbouring site, that is eight different diffusion processes in total, namely two types of particles times two types of starting sites times two types of destination sites. Lastly, we have four reaction processes in our model, using either of the two types sites for the O involved and either of the two types of sites for the CO. The CO₂ formed in a reaction is modeled to disappear from the surface immediately by associative desorption.

2 CO oxidation on Pd(100)

2.1 Lattice structure

The catalyst used in this study is Pd(100), or actually the Pd(100)($\sqrt{5} \times \sqrt{5}$) $R27^\circ$ oxidized restructured top layer. In figure 1 this surface is shown. On the right-hand side of figure 1a we find the clean Pd(100) crystal, on the left-hand side the restructured top layer is shown. This surface has quite a few different types of adsorption sites, of which we will only consider two. These two are called hollow sites and bridge sites. Which are those are visible in figure 1b.

Remark from figure 1 that in the pure oxide, that is, not in reaction conditions, all of the hollow sites are occupied by oxygen atoms and the bridge sites remain empty.

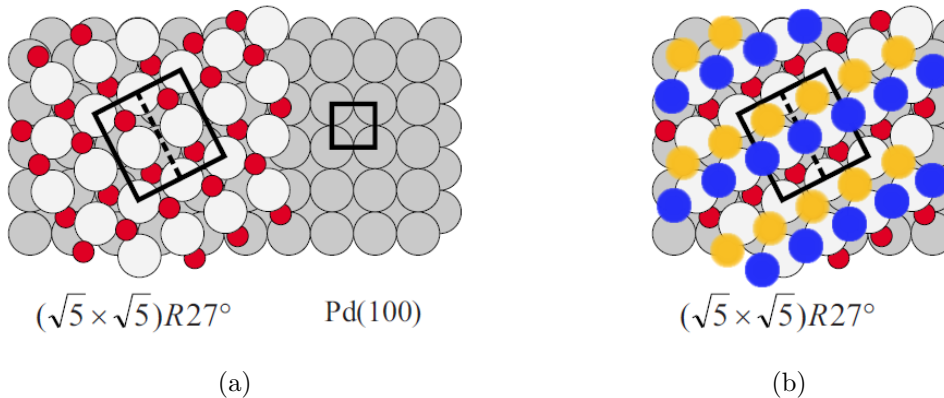


Figure 1: Figure 1a [9] depicts the surface that we are investigating. The far left side shows the $(\sqrt{5} \times \sqrt{5})R27^\circ$ oxide structure. The light gray spheres are palladium atoms of the oxidized layer, the red spheres are oxygen atoms and the dark gray spheres are palladium atoms of the lower bulk layers. The black squares depict the $\sqrt{5} \times \sqrt{5}$ restructured unit cell and the 1×1 cell of the bulk. Picture 1b shows the hollow sites (orange spheres) and bridge sites (blue spheres). Remark that the top most oxygen atoms of the oxide are included in the lattice and the lower layer of oxygen is not.

2.2 Role of oxide

It has already been shown [3, 13] that transition between a rough metal surface and an oxidized surface has a large influence on the reaction rate of oxidation. During reaction at the oxide, the oxygen is removed from the surface and the palladium atoms become mobile. This roughens the surface which, when rough enough, flips to a metal state. In this metal state CO is believed to stick to the rough parts. In this phase the reaction smoothens the surface which at a critical point becomes oxidized again, thus producing a cycle in the surface structure. This cycle is proposed to be responsible for the oscillations in the reaction rate. Experiments have indeed shown that the reaction rate is lower for the metal phase than for the oxide phase.

In this study we have only looked at the oxidized surface. We have specifically studied the amount of oxygen present on the surface, in particular on the hollow sites since these are the oxygen atoms that are part of the oxidized layer. We have tried to gain information on the processes happening while the surface roughens.

3 Kinetic Monte Carlo

The natural mathematical framework to work with the kind of systems we study here is the language of interacting particle system. This area of mathematics is used for example to model diffusion by the so called exclusion process. However here we have twenty-two interacting processes and as such trying to exactly calculate the time evolution of the catalytic system is not possible. While the exclusion process can be used to model a single diffusion process for a single type of particle, we now stand empty-handed for our system involving two types of particles, two types of sites and twenty-two different possible processes altogether. A different approach is therefore necessary. This approach will be to use the kinetic Monte Carlo method to stochastically describe the system. The section below gives a brief overview of the method.

The algorithm of a kinetic Monte Carlo simulation is basically that of a regular Monte Carlo simulation in the sense that a random number is chosen based on the current state of the system in order to evolve it to the next state. [14] This is then iterated so one can find the state the system converges to (if any) without doing the tedious or even impossible calculations. The difference with regular Monte Carlo is that in kinetic Monte Carlo we also keep track of a ‘physical’ time in which the modelled processes take place so that the interacting processes take place in their own time scale. Not only does this guarantee that speedier processes happen more often, i.e. with higher probability in each step, it also gives us a posteriori information of the speed at which the state might undergo structural changes.

A way to say the same thing in a different language is to consider Markov chains. The state of the system as described above is taken as an element of a state space and the random parameter chosen directs the system to a new element of the state space. Indeed the parameter that we choose only depends on the current occupations of the surface sites involved. In this way the evolution of the surface changes to a continuous time Markov process in which the time steps are determined by the random parameter and thus by the current state itself.

3.1 Choosing a process

In order to choose at each simulation step by which process the system will be updated, we need to impose some information on the time dependence of each of the processes involved such that the faster processes have a higher probability of being chosen. We’ll give each lattice site several exponential clocks, one for each possible process. This means that the time it takes for process i to occur at site j is given by a random variable T_{ij} with exponential distribution $Exp(k_{ij})$, where k_{ij} is called the rate for process i at site j . The time for anything to happen at site j is then the minimum over i of these T_{ij} ’s. We know from probability theory that this minimum is again exponentially distributed. This is easily proven by noting that these processes are independent and using the property $e^x \cdot e^y = e^{x+y}$ of the exponential map. The rate is thus the sum over the individual rates, i.e.,

$$T_j = \min_i T_{i|j} \sim \text{Exp} \left(\sum_i k_{ij} \right)$$

We can lift this one step higher, by using the same argument to show that the time it takes for anything to happen anywhere will again be exponentially distributed

$$T_{\min} = \min_{i,j} T_{ij} = \min_{i,j} T_{i|j} \sim \text{Exp} \left(\sum_{i,j} k_{ij} \right)$$

Choosing a process and a site then comes down to first picking the site and then picking the process. For this it is customary to divide the unit interval in weighted shares, picking a

uniformly random number in the interval and checking which site, or in the second step, which process the subinterval that this number contains belongs to.

3.2 Handling the time parameter

In each step we update the time by setting $t \mapsto t + \frac{\log(1/\rho)}{\sum_{i,j} k_{ij}}$ where ρ is uniformly distributed on the interval $[0, 1]$. That this is correct is shown as follows. We know that the minimal time is exponentially distributed with parameter $\sum_{i,j} k_{ij}$, and that the cumulative distribution function for the exponential distribution with parameter μ is

$$F(x) = P(X \leq x) = 1 - \exp(-\mu x),$$

which has inverse

$$F^{-1}(u) = \min\{x : P(X \leq x) = u\} = -\frac{1}{\mu} \log(1 - u) \text{ for } u \in (0, 1).$$

Now $u \sim \text{Unif}(0, 1)$ and $1 - u \sim \text{Unif}(0, 1)$ are equivalent, so we find $-\log(u)/\mu \sim \text{Exp}(\mu)$. Inserting $\mu = \sum_{i,j} k_{ij}$ completes the proof of the claim.

3.3 The rates

We have not yet determined the rates for each of the processes being modeled. Formulas to calculate these are quite common, but they require knowledge of the values of the energies involved in each of the processes. These have been taken from density-functional theory calculations performed by Rogal et al. [9]

A remark we should make in order to avoid confusion is that for adsorption the pressure is already included in the formula. As such these are actual rates instead of rate constants.

3.3.1 Formulas

For each of the rates the partial pressures P_{O} and P_{CO} of oxygen (O_2) and CO and the temperature T of the surface are of importance. As is customary in physical literature we use k_B for Boltzmanns constant and h for the reduced Planck constant.

Now the rates found in [9] are

$$k_{i,j}^{\text{ads}} = f_{i,j}^{\text{ads}}(T) \frac{p_i A_i}{\sqrt{2\pi m_i k_B T}} \exp\left(-\frac{\Delta E_{i,j}^{\text{ads}}}{k_B T}\right) \quad (1)$$

$$k_{i,j}^{\text{des}} = k_{i,j}^{\text{ads}} \exp\left(-\frac{\Delta\mu(p_i, T) - E_{i,j}^{\text{bind}}}{k_B T}\right) \quad (2)$$

$$k_{i,j}^{\text{diff}} = f_{i,j \rightarrow k}^{\text{diff}}(T) \left(\frac{k_B T}{h}\right) \exp\left(-\frac{\Delta E_{i,j \rightarrow k}^{\text{diff}}}{k_B T}\right) \quad (3)$$

$$k_{\text{O}_j + \text{CO}_k}^{\text{reac}} = f_{\text{O}_j + \text{CO}_k}^{\text{reac}}(T) \left(\frac{k_B T}{h}\right) \exp\left(-\frac{\Delta E_{\text{O}_j + \text{CO}_k}^{\text{reac}}}{k_B T}\right) \quad (4)$$

The subscripts are to be interpreted as follows: the subscript i is used to denote a particle of type i , i.e. CO or O and the subscripts j and k are used to denote the type of site that a particle is on or to which it jumps. Furthermore A_i is the effective sticking area, m_i is the mass of a particle of

type i and the different f 's are prefactors which may depend on temperature. The prefactor for adsorption determines the fraction of particles approaching the surface in the correct direction and the prefactors for diffusion and reaction give the ratio between the vibrational part of the partition functions of the transition state and the initial state. These are assumed not to differ much and as such the f -prefactors will be taken to be unitary.

The ΔE 's are the energy barriers involved in each of the processes and $E_{i,j}^{\text{bind}}$ is the binding energy of particle i at site j .

Lastly, we find $\Delta\mu$ in the desorption formula. This is the difference in the chemical potential between the adsorbed phase and the surrounding phase. For this too we can give an expression [7]

$$\Delta\mu(p, T) = -k_B T \log \left[\left(\left(\frac{2\pi m k_B T}{h^2} \right)^{3/2} \frac{k_B T}{p} \right) \left(\frac{k_B T}{\sigma B_0} \right) \left(1 - e^{\hbar\omega_0/k_B T} \right) I_{\text{spin}} \right],$$

where the σ the (classical) symmetry number, B_0 the rotational constant, ω_0 the ground state vibrational frequency and I_{spin} the electronic spin degeneracy of the ground state are particle specific parameters.

Combining equations (1), (2) and the expression for $\Delta\mu$ we find for the desorption rate:

$$k_{i,j}^{\text{des}} = f_{i,j}^{\text{ads}}(T) \frac{2\pi m I_{\text{spin}} A_i}{\sigma B_0} \left(\frac{k_B T}{h} \right)^3 \left(1 - e^{\hbar\omega_0/k_B T} \right) \exp \left(-\frac{\Delta E_{i,j}^{\text{ads}} - E_{i,j}^{\text{bind}}}{k_B T} \right).$$

Remark that the pressure drops out of the equation, which is exactly what one would expect. The pressure is of importance for the location of the equilibrium between adsorption and desorption, but only acts on the adsorption side of the equation.

3.3.2 Values

The values of the parameters σ , B_0 , ω_0 and I_{spin} can be found in chemical and physical tables [11] and the value for the A_i 's is given in [9]. They are listed below.

| parameter | value for O/O ₂ | value for CO |
|-------------------|----------------------------|--------------------------|
| σ | 2 | 1 |
| B_0 | 1.445 cm ⁻¹ | 1.9302 cm ⁻¹ |
| ω_0 | 1580.246 cm ⁻¹ | 2169.52 cm ⁻¹ |
| I_{spin} | 3 | 1 |
| A_i | 6.49 Å | 9.74 Å |

Table 1: Values for the particle specific parameters for both oxygen and CO.

The values of the energy parameters and the effective sticking surface come from Rogal et al. [9] The energy barriers are calculated by density-functional theory calculations by Rogal et al. We list them below. All energies are in eV.

Adsorption: The adsorption energy barriers were found to be non-existent in most cases. Only in the case of adsorption of oxygen on two bridge sites, a quite large adsorption barrier was found.

| particle | site(s) | ΔE^{ads} |
|----------|---------|-------------------------|
| O-O | br-br | 1.9 |
| O-O | hol-hol | 0.0 |
| O-O | br-hol | 0.0 |
| CO | br | 0.0 |
| CO | hol | 0.0 |

Table 2: Energy barriers for each adsorption process. Each energy is in eV.

Desorption: The binding energy is a bit more difficult since it depends on neighbouring particles too, both on the type of particles and the type of sites these particle occupy. The total binding energy can be calculated as $E^{\text{bind}} = E_0^{\text{bind}} + 2U$ where E_0^{bind} is a constant part and U is the neighbour interaction part. Both are found in the tables below.

The constant part is

| particle | site(s) | E_0^{bind} |
|----------|---------|---------------------|
| O-O | br-br | -1.02 |
| O-O | hol-hol | -3.90 |
| O-O | br-hol | -2.46 |
| CO | br | -1.40 |
| CO | hol | -1.92 |

Table 3: Constant parts of the binding energies in eV.

and the neighbour interaction part can be calculated as

$$U = \sum_{l: \text{neighbours}} n_l V_l.$$

Here the n_l 's specify the number of neighbours of type l , i.e. the type of site and the type of particle and the V_l 's are the corresponding neighbour interaction energies. The values for the V_l 's are given below.

| particle | sites | V |
|----------|---------|------|
| O-O | br-br | 0.08 |
| O-O | hol-hol | 0.07 |
| O-O | br-hol | 0.08 |
| CO-CO | br-br | 0.08 |
| CO-CO | hol-hol | 0.13 |
| CO-CO | br-hol | 0.14 |
| O-CO | br-br | 0.06 |
| O-CO | hol-hol | 0.11 |
| O-CO | br-hol | 0.13 |
| O-CO | hol-br | 0.12 |

Table 4: Neighbour interaction parts of the binding energy. These enter both in the rates for desorption and diffusion. Again these are in eV.

Diffusion: Diffusion too depends on the number and type of neighbours of the involved sites. This dependence is as follows. For diffusion of a particle of type i from site j to site k one has an energy barrier of $E_{i,j \rightarrow k}^{\text{diff}} = E_i^{\text{diff}} + U_{j \rightarrow k}$ where we have

$$U_{j \rightarrow k} = \max \left\{ 0, \sum_{l: \text{neighbours of } k} n_l V_l - \sum_{l: \text{neighbours of } j} n_l V_l \right\}.$$

This parts seems overly complicated but it is just the extra energy barrier provided by a possibly larger neighbour interaction. The constant part E_i^{diff} is

| particle | diffusion | $E_i^{\text{diff}}_0$ |
|----------|-----------|-----------------------|
| O | br → br | 1.2 |
| O | br → hol | 0.1 |
| O | hol → br | 1.54 |
| O | hol → hol | 1.4 |
| CO | br → br | 0.4 |
| CO | br → hol | 0.3 |
| CO | hol → br | 0.82 |
| CO | hol → hol | 0.6 |

Table 5: Constant parts of the diffusion energy barriers in eV.

Reaction: The reaction energies are again straightforward. There is no added neighbour interaction, thus we can just list the entire energy barriers in the table below.

| site O | site CO | ΔE^{reac} |
|--------|---------|--------------------------|
| br | br | 1.0 |
| br | hol | 0.5 |
| hol | br | 0.9 |
| hol | hol | 1.6 |

Table 6: Energy barriers for the possible reactions in eV.

4 Results of Rogal, Reuter and Scheffler

In the same paper [9] from which we have extracted the values for the energy barriers, Rogal et al. describe their kinetic Monte Carlo simulations. They compare their results with earlier studies that have given the structure of the surface in a wide range of partial pressures of both oxygen and CO.

Figure 2 shows the surface structure that they have found and figure 3 shows the occupation of hollow sites by oxygen as a function of the partial CO pressure at fixed oxygen pressure and three fixed temperatures. It turns out that their kinetic Monte Carlo simulations agree with their earlier calculations of the structure of the palladium. [8]

Figure 4 shows that the oxygen that is removed from the hollow sites is replaced with CO particles. This is exactly what we will see later on in this study as well.

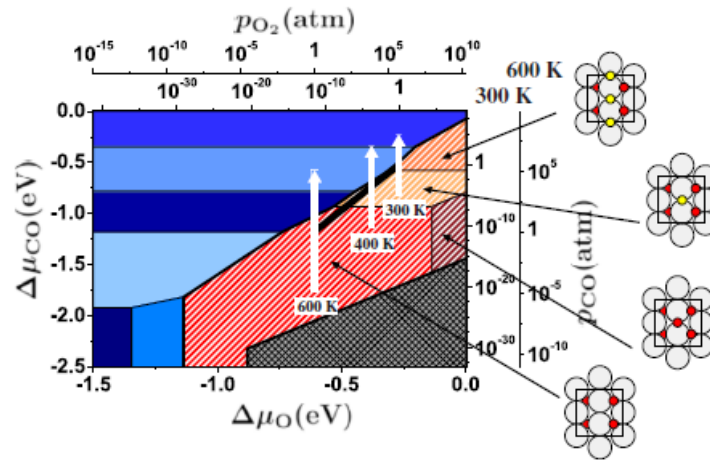


Figure 2: This figure [8] shows the structure of the palladium as a function of the oxygen pressure (horizontal axes) and the CO pressure (vertical axes). The left and bottom axes give the values for the chemical potential for each of the pressures on the right and top axes. The left and top axes give double values, one for $T=300\text{K}$ and one for $T=600\text{K}$. Each of the regions represents a different state of the palladium or palladium oxide. The red parts are of interest of us; these are the regions in which the $(\sqrt{5} \times \sqrt{5})R27^\circ$ structure exists. The small pictures next to the diagram depict schematically what sites are occupied by what atoms. Red atoms are oxygen while yellow ones are CO.

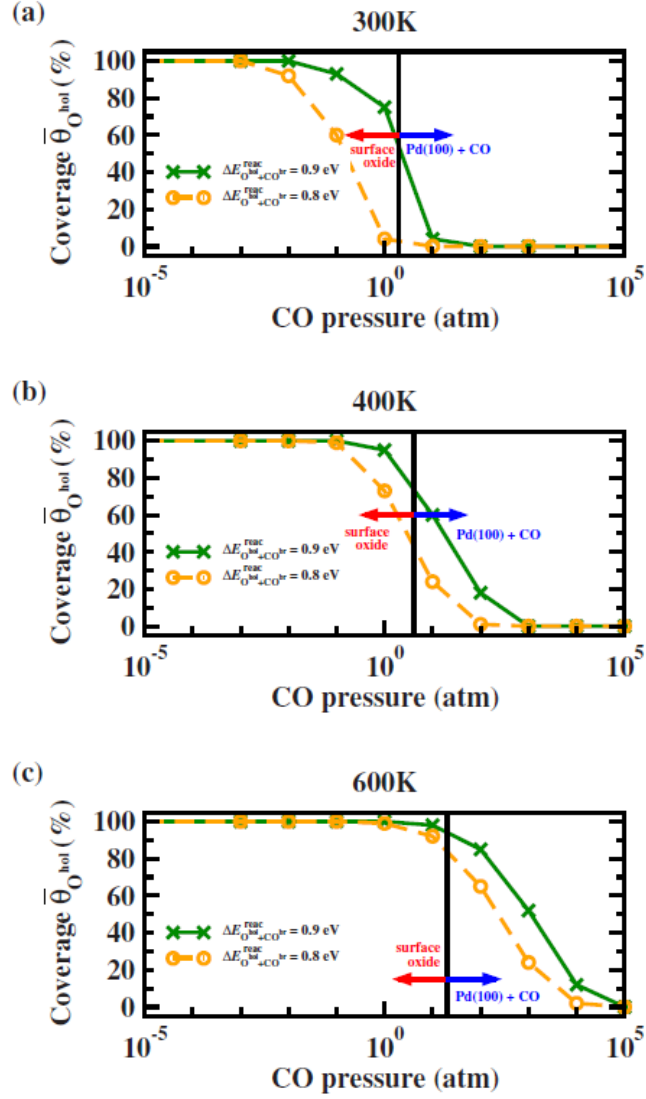


Figure 3: Results of the entire simulation run by Rogal, Reuter and Scheffler [9]. In each of the graphs the horizontal axis shows the pressure of CO. The oxygen pressure was fixed at $p_O = 10^5$ Pa for each. The vertical axes show the time-averaged fraction of sites occupied by oxygen. The temperature is (a) $T=300$ K, (b) $T=400$ K and (c) $T=600$ K. The green lines are found by setting the value of the reaction rate for oxygen from hollow and CO from bridge sites as set in Table 6. The yellow lines are found for a slightly different energy barrier of 0.8 eV. The vertical black lines are the boundaries from the red region to the blue region in figure 2.

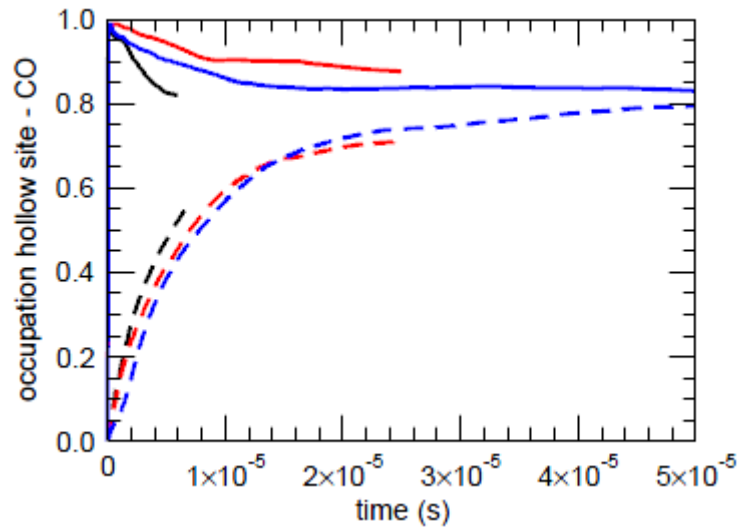


Figure 4: This figure [6] is complementary to figure 6. It shows the fraction of hollow sites covered by CO during the simulation run. The temperature is $T=600\text{K}$ and the pressures are $p_{\text{O}} = 1 \text{ atm}$ and $p_{\text{CO}} = 10^4 \text{ atm}$. The lattice size is 20×20 . Both simulations from an empty surface (solid lines) and a surface filled with oxygen on the hollow sites (dotted lines) are shown. The convergence of these simulations is discussed below. See section 5.1.

5 Simulations

In each of the simulations we have used a lattice of 14x14 sites (98 bridge sites and 98 hollow sites) with periodic boundary conditions. For each of the sites we have to keep track of which sites are its neighbours and what are the rates for each of the different processes. For this the data is stored in a three dimensional array, of which each plane has its own purpose. The bottom plane is filled with either 0 for an empty site, 1 for a site covered with oxygen and -1 for a site covered with CO. Then there are twenty-two planes storing the current rates and a plane which stores the sum of rates for each site for computational purposes. Which sites are neighbours is determined by a separate function since the surface sites form a hexagonal pattern while the array forms a square pattern so extra information is necessary.

In the above the rates in the array are referred to as current rates. The reason for this is that most of the rates depend on the type and number of neighbours a site has. For example adsorption of oxygen is prohibited if an empty site has no empty neighbours and the rate is set to zero. Another example is desorption of any type of particle since the binding energy depends greatly on the number of neighbours.

An important detail that should be mentioned is that the diffusion rates also depend on the neighbours of the destination site. To keep track of this correctly, one should reserve a plane in the array for diffusion in each direction. In the simulation this was neglected and only a single plane was taken for the rates for each type of diffusion (e.g. CO from bridge to hollow) and a standard direction was chosen to count the number and specify the type of neighbours of the destination site. This embodies an assumption of isotropy in the occupation of the surface. One could argue whether or not this is the correct choice.

In the simulations we have used temperatures in the range of 300 kelvins to 600 kelvins, usually with the temperature either set to 300 K, 400 K or 600 K. The partial oxygen pressure was kept fixed at $p_O = 10^5$ Pa and the partial CO pressures ranged from 1 Pa to 10^{10} Pa.

5.1 Full model

By the full model we refer to the model in which we have five adsorption processes, five desorption processes, eight diffusion processes and all four reaction processes. The f -prefactors from the formulas are approximated as 1 and drop from the equation. Just as these prefactors, the $1 - \exp(-\hbar\omega_0/k_B T)$ factor can very well be approximated as 1 for the temperatures of our interest.

The first aim of the project was to reproduce the results of Rogal et al. For this we needed to find out when one could call the system to be in an equilibrium. For this several starting conditions were tried of which starting with a completely empty surface (i.e. all bridge sites and hollow sites unoccupied) and starting from a surface where the hollow sites were filled with oxygen and the bridge sites were empty were used most of the times.

Figure 5 shows the results from a simulation starting with an empty surface.

The running time of the algorithm implemented is unfavourable. About 10^7 kMC steps could be taken by setting up a simulation on Friday afternoon and ending it on Monday morning. That this is not enough to reach equilibrium can best be seen in figure 6, which shows three simulations by Rogal et al. [6]. The horizontal axis shows the physical time each of the simulations represented. The vertical axis represents the occupation of hollow sites by oxygen. Three different iterations of their algorithm are shown. Convergence is only approximated after roughly 10^{10} steps in the kMC setup. We must remark that their lattice was twice as large as the one used in this study, but this is still such a large difference that a new approach must be

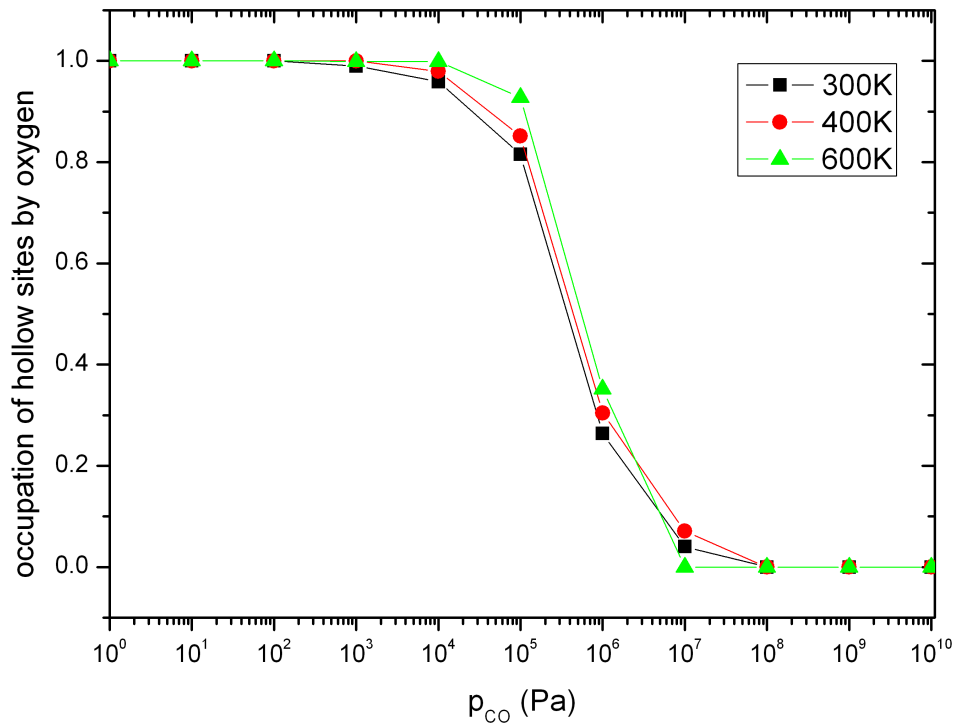


Figure 5: This figure shows the results from an early run of the full model starting with an empty lattice. On the horizontal axis the partial CO pressure is shown. The vertical axis gives the time-averaged fraction of hollow sites occupied by oxygen. Each of the datapoints is simulated with 10^4 kMC-steps. We will see that this is a very small number. The black line gives the result for $T=300\text{K}$, the red line for $T=400\text{K}$ and the green line for $T=600\text{K}$. Note that they almost overlap while the steep part for higher temperatures should lie further to the right according to the data by Rogal et al.

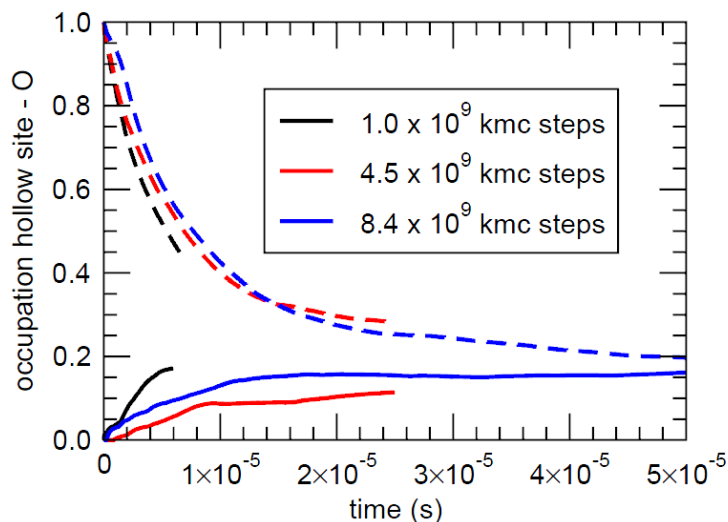


Figure 6: This figure [6] shows convergence in the simulations run by Rogal et al. As usual the vertical axis depicts the fraction of the hollow sites covered by oxygen. The horizontal axis shows the physical time represented by the simulations. It is shown that several tries were necessary to approximate convergence. The lattice size is 20×20 , that is 200 hollow sites and 200 bridge sites. The temperature is 600 K, the oxygen pressure is 1 atm and the CO pressure is 10^4 atm. The solid lines are from a simulation starting with an empty lattice. The dotted lines depict simulations that started with the hollow sites filled by oxygen and the bridge sites empty.

investigated. This can be understood clearest especially if one keeps in mind that these 10^{10} steps were necessary for a data point of only a single CO pressure and a single temperature. To find data like in figure 3 one would have to do thirty of these experiments.

Figure 7 gives the relation between the CO pressure and the physical time of a simulation. We notice that the time represented in a simulation depends strongly on the pressure of CO. This means that the above claim can be weakened by stopping after a certain physical time has passed. This means that not all of the thirty datapoints would have to take as long, but already a single one would already mean an enormous running time.

5.2 To study the rarer processes

The main cause for the very slow convergence is the fact that adsorption and desorption of CO give a lot of noise in the following sense. Since the desorption rate of CO – in particular from the bridge sites – is several orders of magnitude larger than the rates for the other processes, a CO particle on a bridge site is very likely to desorb. Conversely, the adsorption rate for CO is also very large, in part due to the absence of an energy barrier. As a consequence adsorption and desorption of CO quickly follow each other and other processes rarely happen. This is not strange as the physical timescales of this kind of simulations are very small; this both follows from the large rates (remember that time is updated with $1/\sum k$) and is observed in the simulations (see figure 7). Because of this one would not expect to see the rare processes often –so there is no problem there– but this does produce simulations that have to run an extreme number of steps in order for anything interesting to happen.

Remark that the adsorption rate for oxygen on at least one hollow site does not differ much from that for CO on either site. The reason that we see adsorption of CO that much more often than adsorption of oxygen is simple: for oxygen we need to have two sites available while CO only

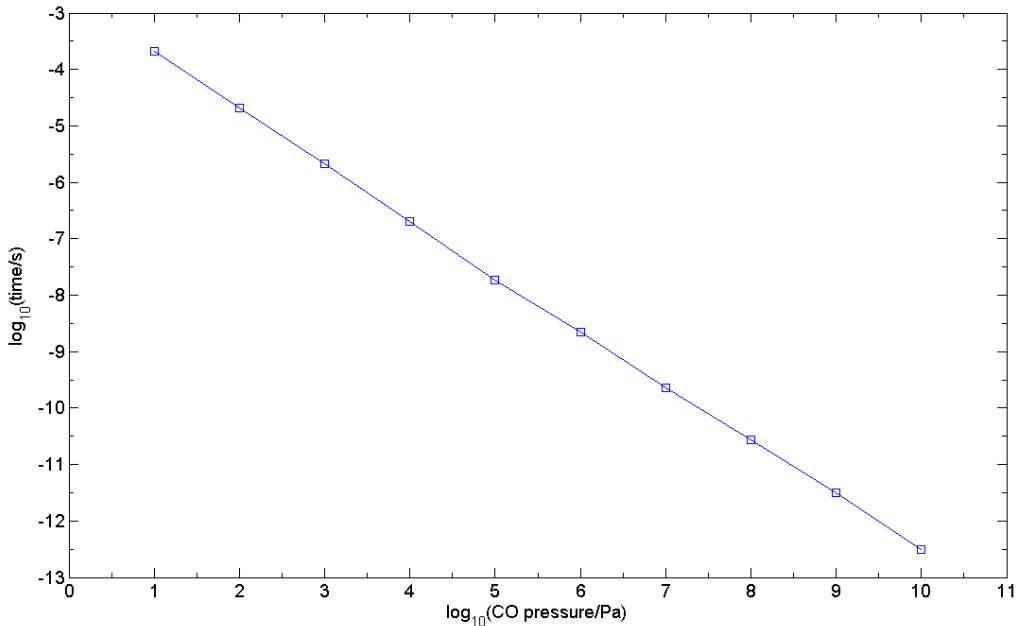


Figure 7: This figure gives the relation between the CO pressure and the physical time of a simulation. The particular curve is at $T=300\text{K}$ and 10^4 kMC steps at a fixed oxygen pressure of 10^5 Pa. Higher pressure makes for a simulation that represents less time with the same number of iteration steps. This is to be expected since the adsorption rate for CO grows linearly with pressure and the time decreases with the sum of rates. As the possible restructuring happens at high CO pressures this is unfavourable for our purposes.

needs one. We usually have ample bridge sites available, but adsorption of oxygen on bridge sites was precisely the one with a high energy barrier!

5.2.1 Handling CO and problems

A way to get a hold on the rarer processes is to shut off the common ones. This does mean that we have to artificially impose some condition on the system that would otherwise evolve from these turned off processes. The processes that we shut off are adsorption and desorption of CO on both bridge sites and hollow sites and the diffusion of CO between bridge sites. The information we impose on the system is the coverage of CO on bridge sites. Using figure 2 for each pressure of CO we read off the fraction of bridge sites that ought to be covered by CO in equilibrium. Now during a simulation after every ten kMC steps we take the bridge sites at which no oxygen is adsorbed and either fill it with CO or let it be empty with a probability equal to the fraction of sites that should be covered. The bridge sites covered by oxygen are kept intact as not to stir up the processes that are still switched on. Remark that this way of distributing CO over the bridge sites not only accounts for the adsorption and desorption but also for the shut off diffusion.

Also the CO on the hollow sites was kept intact since we try to retrieve the amount of oxygen on these sites and as such cannot impose a condition on the fraction of these sites covered by CO as this would suggest a priori knowledge of these sites.

This way of working does yield a significant disadvantage in that it is now difficult to remove CO from hollow sites. The only processes left capable of that are 1. the reaction of CO from a hollow site with O from a hollow site, with a high energy barrier; 2. the reaction of CO from a

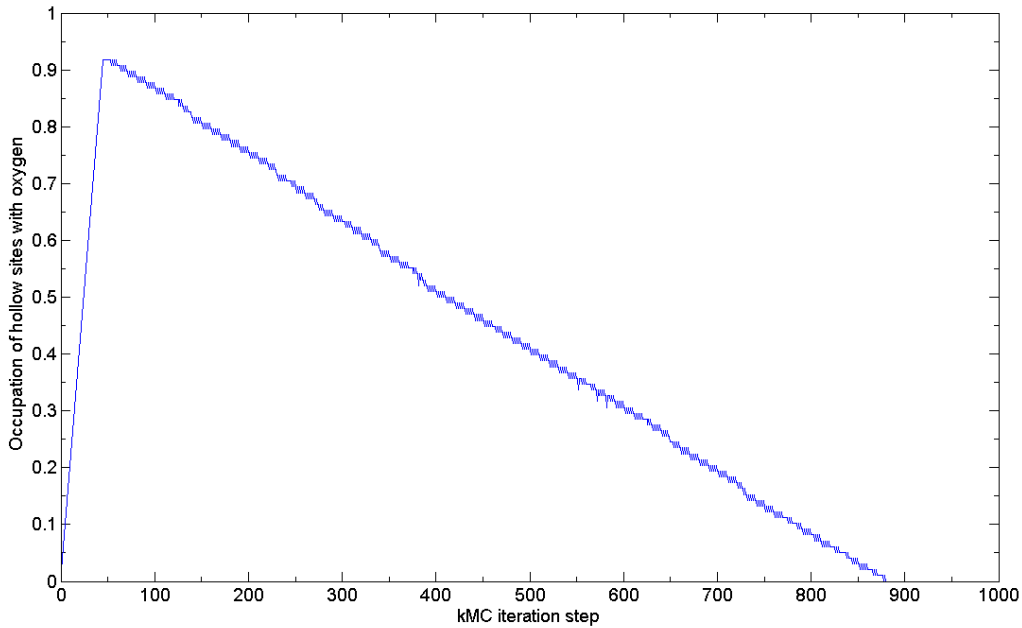


Figure 8: This figure shows the fraction of hollow sites occupied by oxygen throughout the simulation where the common CO processes are shut off. This specific simulation was set up from an empty surface at $T=300\text{K}$ and a CO pressure of 10^8 Pa. The horizontal axis shows the iteration step of the kMC algorithm. We see some oscillations produced by adsorption and desorption of oxygen from a hollow site plus a bridge site and every now and then a more permanent step downwards produced by a reaction of oxygen from a hollow and a CO from a bridge site followed directly by diffusion of CO from a bridge site to afore mentioned hollow site. The entire simulation is terminal since the processes capable of removing CO from a hollow site are unlikely because either the energy barrier is very large or the proper conditions are rare. Because of this the CO poisons the hollow sites. In this simulation this poisoning has happened after a little under 900 kMC steps.

hollow site with O from a bridge site, which has a relatively low energy barrier but does require a rare oxygen atom on a bridge site; and 3. diffusion of CO from a hollow to a bridge site. As such the CO particles on hollow sites are very rarely removed which eventually poisons the hollow sites since oxygen is more easily removed from these.

This way of working does however yield some interesting information. In figure 8 we see the coverage of oxygen oscillates for a bit and every now and then drop a unit part. These drops coincide with a reaction of an oxygen particle with a CO particle from a bridge site quickly followed by diffusion of a second CO particle from a neighbouring bridge site to steal the position of the formerly adsorbed oxygen particle. The oscillations are produced by adsorption and desorption of oxygen from a hollow site and a bridge site. From this we conclude that the diffusion of CO is important for the depletion of oxygen from hollow sites.

A problem that should not go unmentioned is that two simulations starting from the same initial conditions can show entirely different behaviour. A second plot of the kind in figure 8 is found in figure 9 where we also see the general behaviour of oscillations and the incidental drop by reaction and diffusion as described above, but where these drops are a lot less common. For this no explanation was found.

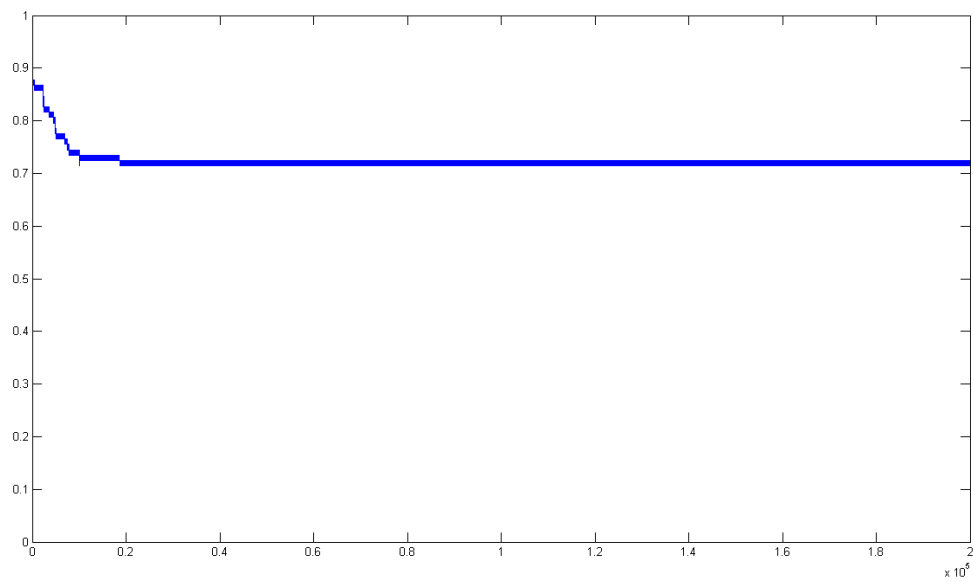


Figure 9: Like figure 8 this figure shows a run of the simulation where the common CO processes are shut off. The same starting conditions are applied. Indeed we have an empty stating surface even though this is not clear because of the scale on the horizontal axis. This simulation is ended after 200,000 kMC steps. Here too we see the oscillatory behaviour of adsorption and desorption of oxygen while the steps downwards by reaction happen a lot less frequently. We offer no explanation for the difference in the two runs.

6 Intermezzo: The entropy effect

A natural question one may ask oneself is whether the details of the specific processes even matter for the general result. The process we are dealing with is in its core one of occupied and vacant sites. In this section we will discard any knowledge we have on the specific properties of sites occupied by oxygen, those occupied by carbonmonoxide and those remaining empty. We'll only distinguish between occupied by either oxygen or CO and calculate the contribution this gives us on the entropy. Denote with N the number of total sites on some large area, and with k the number of sites covered by CO on this same area. Thus we have $k \leq N$.

Let the sites occupied with CO be randomly distributed. Then the entropy of this configuration is given by $S = k_B \log W$, with $W = \binom{N}{k}$. Since we have taken a large area, N is large. We'll assume for the moment that also k and $N - k$ are large. This justifies using Stirlings approximation in calculating the entropy. We find

$$\begin{aligned}
 S/k_B &= \log \binom{N}{k} \\
 &= \log N! - \log k! - \log(N - k)! \\
 &\approx N \log N - N - k \log k + k - (N - k) \log(N - k) + (N - k) \\
 &= N [\log N - \log(N - k)] + k [\log(N - k) - \log k] \\
 &= N \log \frac{N}{N - k} + k \log \frac{N - k}{k}
 \end{aligned}$$

If we now are interested in a decrease of ten percent in the oxygen covering of hollow sites, we simply take $k = 0.1N$. Then the entropy is given by $S/k_B \approx N \log \frac{9}{10} + \frac{1}{10}N \log 9 \approx 0.11 \cdot N$. When we now consider the entropy per site at a temperature range that we're interested in, we find $ST/N \approx 5.9$ meV at $T=600$ K. This of course is so much smaller than the energies involved that we can conclude that solely the contribution of entropy is not enough to destabilize the system.

7 Reducing the model

We'll now discuss the second way in which we have tried to get a hold on the interesting processes, namely by stripping away some processes and not simulating but using differential equations. For this we calculated the rates for several different temperatures and CO pressures and checked which were in the range of the reaction rate for oxygen from hollow sites with CO from bridge sites. Most of the diffusion processes turned out to be extremely quick (and a few extremely small). Because of this we assume that the particles are spread out over the surface and forget the local structure. Off course, we can only do this for diffusion processes which have the same initial and final type of site. This indeed allows us to set up differential equations. The processes that we take into account for these are:

- adsorption and desorption of CO on bridge sites
- adsorption and desorption of CO on hollow sites
- adsorption and desorption of O₂ on two hollow sites
- adsorption and desorption of O₂ on a bridge and a hollow site
- diffusion of O from bridge to hollow sites
- diffusion of CO from bridge to hollow sites and vice versa
- reaction of O from bridge with CO from hollow
- reaction of O from hollow with CO from bridge (the interesting reaction)

These are now only thirteen processes left. Also because we have forgotten the local structure this becomes easier to handle since solving a small system of differential equations is easier than using the language of interacting particle systems.

Note that we have taken into account some adsorption or desorption processes that just based on the rates (not shown) we would not have to. However, each adsorption process should be paired with its accompanying desorption as not to poison the surface as in section 5.2.1.

7.1 Further simplification

Now we'll strip even more processes away. Diffusion of oxygen from bridge sites to hollow sites does have a relatively large rate. But since oxygen rarely occupies a bridge site, we do not expect to make a large mistake by taking it away. Also the diffusion parameter of CO from bridge to hollow sites is 10⁴th to 10⁹th times larger than the diffusion rate from hollow to bridge, depending on the temperature where for higher temperatures this factor is smaller than for lower temperatures. We therefore pack these two processes together in a resulting diffusion from bridge to hollow. In the equations we have used the rate of this diffusion without a correction since the difference between the two rates is so large.

Figure 10 shows a schematic of the system now under study. The left-hand part of the schematic and the right-hand part are almost decoupled. The only coupling between the two is the adsorption and desorption of O₂ on hollow and bridge sites and the diffusion of CO from bridge to hollow sites. This first coupling is very weak since the bridge sites are known to be mostly empty. This means that the adsorption process can be seen as adsorption of a single O atom on a hollow site. The desorption then also becomes desorption of a single O atom. The effective rates for this are unknown but as the requirement of an empty bridge site is not a heavy one we just use the normal rate for the dissociative desorption of O₂ on the hollow and bridge site together. And as we still require the same balance between adsorption and desorption this also

determines the effective desorption rate.

Now the only coupling left between the left-hand and right-hand sides is the diffusion. In order to say something about its importance to the catalysis, we just leave it away and see how the system behaves.

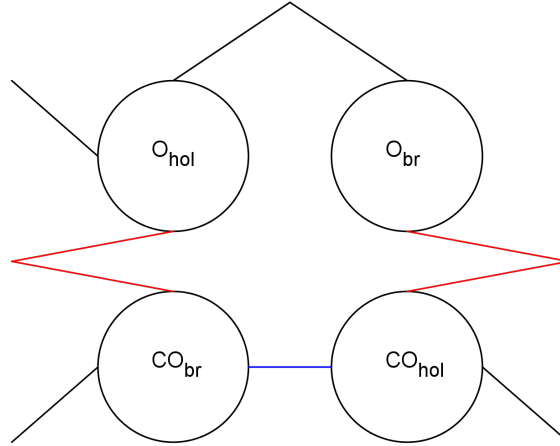


Figure 10: This schematic shows the processes left in the model after stripping away the fast diffusion and the extremely rare processes. Black lines indicate adsorption and desorption, the red line indicate reaction of oxygen and CO and the blue line is the diffusion of CO from bridge to hollow sites.

7.2 Differential equations

Let x be the fraction of hollow sites covered by oxygen and y be the fraction of bridge sites covered by CO. The differential equations each of the porcesses give are found in table 7.

| process | equation |
|---------------------------|---------------|
| adsorption O ₂ | $2k_1(1-x)^2$ |
| desorption O ₂ | $-2k_2x^2$ |
| adsorption O | $k_3(1-x)$ |
| desorption O | $-k_4x$ |
| adsorption CO | $k_5(1-y)$ |
| desorption CO | $-k_6y$ |
| reaction | $-k_7xy$ |

Table 7: Contributions of each of the processes to the differential equations.

The complete system of differential equations are now

$$\frac{dx}{dt} = 2(k_1 - k_2)x^2 - (4k_1 + k_3 + k_4)x + 2k_1 + k_3 - k_7xy \quad (5)$$

$$\frac{dy}{dt} = -(k_5 + k_6)y + k_5 - k_7xy \quad (6)$$

The values for the k 's can be calculated with the information from section 3.3.

In order to solve these equations we remark that when we are interested only in the equilibrium solution, then setting $\dot{x} = 0 = \dot{y}$ suffices. From this the mixed term k_7xy is canceled and we are left with an equation quadratic in x and linear in y . Also from \dot{y} alone we find a second

equation in x and y : $y = -\frac{k_5}{k_5+k_6+k_7x}$. Substituting y from the second equation into the first we find the cubic equation

$$\begin{aligned} & \frac{2(k_1 - k_2)k_7}{k_5 + k_6}x^3 \\ & + \left(2(k_1 - k_2) - \frac{(4k_1 + k_3 + k_4)k_7}{k_5 + k_6} \right) x^2 \\ & + \left(\frac{k_7(2k_1 + k_3 + k_5)}{k_5 + k_6} - (4k_1 + k_3 + k_4) \right) x \\ & + 2k_1 + k_3 - 2k_5 \\ & = 0. \end{aligned}$$

Due to time constraints no numerical analysis was performed on this equation in combination of the results found earlier by Rogal et al. [9] A complication in such an analysis would be that the rate constants themselves also depend on x and y by neighbour interaction in the energy barriers. These interactions are quite large in theory. Comparing an analysis of the cubic equation (as a function of temperature and both pressures) and the results by Rogal et al. would give insight in the practical effects of these neighbour interactions.

As a consequence the equations (5) and (6) are not easy to solve. But some numerical analysis can be done with the Matlab function `fsolve` which uses a Newton-like method. This was done for both $T=300\text{K}$ and $T=600\text{K}$. For a temperature of 300 kelvins the location of the fixed point found with Matlab was very unstable, it depended a lot on the initial conditions $x(0)$ and $y(0)$. As we have neither found nor searched for an explanation for this we will not try to conclude anything from it.

For $T=600\text{K}$ the solution did not depend on the initial conditions but it did not depend on the value of the CO pressure either; at least not in the already physically large range of $1 - 10^{10}$ pascals! The solution that was found was $(x, y) \approx (0.98, 0)$. There are several remarks we can make on this result:

- This solution is not what we know of the entire system, there is too much oxygen on the hollow sites and this should certainly depend on the CO pressure. Since only the diffusion of CO towards hollow sites has been taken away without reason, we might conclude that this process is very important.
- It is odd that there is very little CO on the bridge sites. Especially if we again remember that this solution is independent of the CO pressure. At high pressures we already know that there is some CO on the bridge sites, this is exactly what we have used in section 5.2.1.
- The first and second remark seem to conflict. As there is little CO on the bridge sites, little would be able to diffuse to hollow sites.

8 Discussion and outlook

Before coming to the conclusion we should make some remarks about the validity of the model and possible changes one could make to it.

- One could include a Mars-Van Krevelen effect for oxygen on the hollow sites. Measurements have shown [13] that the reaction mechanism in the oxidized phase is mainly the Mars-Van Krevelen mechanism, while Langmuir-Hinshelwood dominates at the metal surface. One could alter the model by including this as a new adsorption process of a single O atom for which no desorption process exists. The difficulty would lie in determining the correct rate for this process. As this would amount to a higher coverage of oxygen on the hollow sites and the results of Rogal et al [9] with the same model correspond so nicely with the structure plot (figure 2), one might guess that the absence of this effect is not too much of a problem.
- A weak point of the simulation is that if the surface destabilizes and restructures, then the assumption on the lattice is no longer valid. Moreover this means that the energy barriers might differ from the ones used in this simulation. In fact all the data used here is only valid in the region of the oxidized surface.
- We have included no information on how fast we expect the palladium atoms to become mobile and as such they are kept fixed to the surface. It is not impossible that the palladium atoms become mobile even before CO takes up the place formerly belonging to oxygen that has reacted away.
- Also one could try to solve the differential equations without splitting the system into two parts such that the CO and oxygen will in fact compete for the same surface sites which is lacking in the method of section 7.
- Another way of extracting information on the less common processes of the simulation is to use the technique of importance sampling. This has not been tried.

9 Conclusion

From the artificial simulation of sections 5.2 and the differential equations of section 7 we can conclude –bearing the remarks above– that the oxygen from the hollow sites is only permanently removed if there is CO competing for these very surface sites. In other words, the oxygen from the hollow sites won't come loose without CO taking their place.

10 Acknowledgements

I am thankful towards both my supervisors, as this research project and this thesis would not be possible without them. I'd like to thank Joost for being very approachable and being altogether very inspiring as a physicist, both during our discussions and during the group meetings. To Evgeny I am grateful for all the times he was willing to listen to me and guide me even though the subject of this thesis really wasn't in his area of expertise.

I especially want to thank Jutta Rogal for answering the questions I posed to her by email and even sending me some of her old data.

References

- [1] R.J. Baxter and P. Hu. Insight into why the langmuir-hinshelwood mechanism is generally preferred. *Journal of Chemical Physics*, 116(11):4379–4381, 2002.
- [2] F. Gao, Y. Wang, Y. Cai, and D. W. Goodman. Co oxidation on pt-group metals from ultrahigh vacuum to near atmospheric pressures. 2. palladium and platinum. *The Journal of Physical Chemistry C*, 113(1):174–181, 2009.
- [3] B.L.M. Hendriksen, S.C. Bobaru, and J.W.M. Frenken. Oscillatory co oxidation on pd(100) studied with in situ scanning tunneling microscopy. *Surface Science*, 552:229–242, 2004.
- [4] C.T. Herbschleb. *ReactorSTM: Imaging Catalysts under Realistic Conditions*. PhD thesis, 2011.
- [5] P. Mars and D.W. van Krevelen. Oxidations carried out by means of vanadium oxide catalysts. *Chemical Engineering Science*, 3, Supplement 1(0):41 – 59, 1954. `je:title;The Proceedings of the Conference on Oxidation Processes;ce:title;.`
- [6] Jutta Rogal. Received through personal correspondence.
- [7] Jutta Rogal and Karsten Reuter. Ab initio atomistic thermodynamics for surfaces: A primer. *Experiment, Modeling and Simulation of Gas-Surface Interactions for Reactive Flows in Hypersonic Flights*, pages 2.1–2.18, 2007. Educational Notes RTO-EN-AVT-142, Neuilly-sur-Seine.
- [8] Jutta Rogal, Karsten Reuter, and Matthias Scheffler. First-principles statistical mechanics study of the stability of a subnanometer thin surface oxide in reactive environments: Co oxidation at pd(100). *Phys. Rev. Lett.*, 98:046101, Jan 2007.
- [9] Jutta Rogal, Karsten Reuter, and Matthias Scheffler. Co oxidation on pd(100) at technologically relevant pressure conditions: First-principles kinetic monte carlo study. *Phys. Rev. B*, 77:155410, Apr 2008.
- [10] B.C. Sales, J.E. Turner, and M.B. Maple. Oscillatory oxidation of co over pt, pd and ir catalysts: Theory. *Surface Science*, 114(2-3):381 – 394, 1982.
- [11] D. R. Stull, H. Prophet, and United States. *JANAF thermochemical tables [electronic resource] / D.R. Stull and H. Prophet, project directors*. U.S. Dept. of Commerce, National Bureau of Standards, Washington, D.C. :, 2d ed. edition, 1971.
- [12] J.E. Turner, B.C. Sales, and M.B. Maple. Oscillatory oxidation of co over pd and ir catalysts. *Surface Science*, 109(3):591 – 604, 1981.
- [13] R. van Rijn. *A Structural View of Pd Model Catalysts: High-Pressure Surface X-Ray Diffraction*. PhD thesis, 2012.
- [14] Arthur F. Voter. Introduction to the kinetic monte carlo method. In Kurt E. Sickafus, Eugene A. Kotomin, and Blas P. Uberuaga, editors, *Radiation Effects in Solids*, volume 235 of *NATO Science Series*, pages 1–23. Springer Netherlands, 2007.